Proceedings of the 2012 IEEE 12th International Conference on Bioinformatics & Bioengineering (BIBE), Larnaca, Cyprus, 11-13 November 2012

Image-based Estimation of Biomechanical Relationship between Masticatory Muscle Activities and Mandibular Movement

Yang Yang[1,2], Kelvin Weng Chiong Foong[1,2], Sim Heng Ong[1,3,4], Masakazu Yagi[5], Kenji Takada[2,6]
[1]NUS Graduate School for Integrative Sciences and Engineering, National University of Singapore
[2]Faculty of Dentistry, National University of Singapore
[3]Department of Electrical and Computer Engineering, National University of Singapore
[4]Department of Bioengineering, National University of Singapore
Singapore 119083, Singapore
[5]The Center for Advance Medical Engineering and Informatics, Osaka University
[6]Department of Orthodontics and Dentofacial Orthopedics, Graduate School of Dentistry, Osaka University
Osaka 5650871, Japan
Email: yang01@nus.edu.sg

***Abstract*—Current techniques for investigating the functional roles of masticatory muscles are not suited to explaining subject-specific biomechanical relationship between mandibular movements and masticatory muscle activities. The aims of this study were to estimate the muscle tensions of subject-specific masticatory muscles in dental occlusion through the three-dimensional morphologic changes (3DMCs) of the muscles, and to explain the subject-specific biomechanical relationship between the mandibular movement and the muscle tensions. One healthy adult subject underwent magnetic resonance (MR) scans of the head at mandibular rest position (M0) and maximum intercuspation (M1). Based on the two sets of MR images, the mandibular movement was measured by the position changes of the mental protuberance of the mandible and the muscle tension from M0 to M1 for each masticatory muscle was estimated by its 3DMCs. The results showed the subject-specific biomechanical relationship between the mandibular movement and the muscle tensions, and the mandibular movement could be explained by these related muscle tensions anatomically and functionally.**

Keywords: Masticatory muscles, muscle tension, mandibular movements, three-dimensional morphologic changes, biomechanical relationship.

I. INTRODUCTION

Masticatory muscles are classified into four groups: masseter muscles (MM), medial pterygoid muscles (MPM), lateral pterygoid muscles (LPM) and temporal muscles (TM). The four muscle groups work together to control the elevation and depression of the mandible for our daily mastication, i.e. the mandibular functions. The electromyographic approach (EMG) [1] and the biomechanical modellings [2] have been used for studying the relationship between the mandibular functions and the masticatory muscles activities. Muscle activities during the mandibular movements were recorded to correlate with the mandibular functions. Although the physiological activities recorded by EMG can reflect the muscle functional activities, how the muscles worked together to achieve the mandibular functions, i.e. the biomechanical relationship, could not be explained by the EMG activities. The biomechanical relationship has been suggested to be more important for clinical practices, such as the diagnosis and treatment of masticatory muscle dysfunction and temporomandibular joint disorder (TMJD). On other hand, the biomechanical modellings have been difficult to be employed for the subject-specific case due to the problem of directly measuring parameters, such as muscle tension direction and magnitude in vivo. However, the three-dimensional morphologic changes (3DMCs) of masticatory muscles during mandibular functional movements can be analyzed to measure the muscle anatomic architectural and biomechanical characteristics [3]. The aims of this study were to estimate the mandibular movement and the muscle tensions of masticatory muscles under dental occlusion case, and to explain the mandibular functions in dental occlusion by using the estimated masticatory muscle tensions for the subject.

II. MATERIAL & METHOD

A. Image Data Acquisition

A normal adult male subject (31 years of age, without any dental problems in clenching and jaw-opened movements) underwent MR scans of the whole head with the mandible at the mandibular rest position (M0) and the maximum intercuspation position (M1), with each scan lasting five minutes. To ensure a stable relationship of the teeth at the M0, an acrylic bite prop was customized for the subject. For the

MR scan at the M1, the subject clenched the mandible with a moderate intensity. The protocol (T1, TE: 5 ms, TR: 11.1 ms, slice thickness: 0.7mm) was carried out with a 1.5 Tesla MR scanner (Signa HDx 1.5T, General Electric). After the MR scans, the two sets of the whole-head MR images were registered by MedINRIA-ImageFusion software [4].

B. Estimation of Masticatory Muscle Tensions

Each masticatory muscle tension (active or passive tension), when the mandible was moved from the M0 to the M1, was estimated by its 3DMCs in this study as Fig. 1 shows.

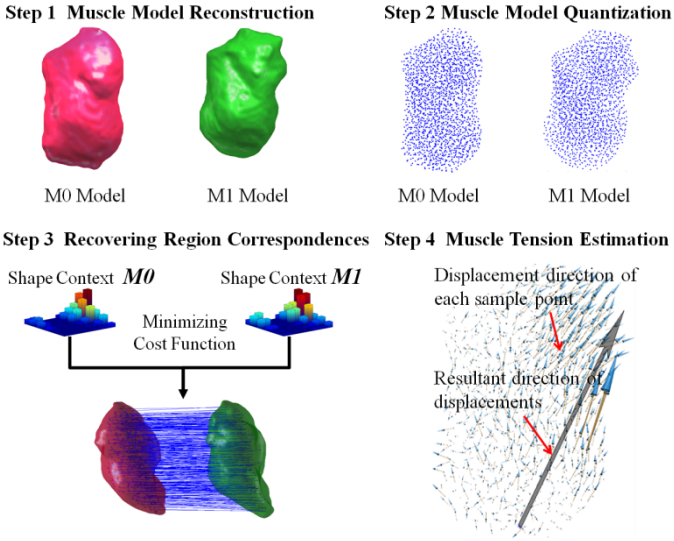

Figure 1. Estimation of Muscle Tension

1) Three-dimensional Reconstruction of Masticatory Muscles: At first, each muscle of the subject was semi-automatically segmented from the two sets of the original MR images by ITK-SNAP software [5]. After the segmentations, a radiologist analyzed and adjusted the anatomic boundaries of the muscle for the anatomic accuracy, and the 3D muscle models of the M0 and M1 positions were reconstructed from these anatomically revised MR images. The inter-rater reliability and the intra-rater reliability of the sixteen muscle segmentations (the left and right muscles at the two mandibular positions) were assessed by the comparisons of the muscle volumes between occasions and between raters using the intraclass correlation coefficient (ICC) as described in [6].

2) Muscle Model Quantization: To numerically describe the 3D morphology of each muscle model and compute region correspondences between the two 3D muscle models (i.e., the M0 model and the M1 model shown in Fig. 1 Step 1) before and after mandibular position changed in Step 3, the large set of voxels in each model was partitioned into specific *K* groups having approximately the same number of voxels nearest to them, and each group was represented by its centroid point (Fig. 1 Step 2). The Lloyd algorithm [7] was employed to achieve the muscle model quantizations.

3) Recovering Region Correspondences: The original shape context method [8] is a rich shape feature descriptor that allows for measuring shape similarity and the recovering of point correspondences in 2D case, and then extended for 3D case by [9]. The 3D shape context has been applied in the non-rigid registration area and biomechanical analysis for the lung surfaces, brain and rat limb skeletons registrations and the strain distribution analysis of rat stomach. In this study, the region correspondences between the M0 model and the M1 model for each muscle were recovered by an extended 3D shape context method as the next three steps describe:

a) Compute the 3D shape context descriptor for each muscle model using the centroid points obtained in Step 2: the original 2D and 3D shape context descriptors were defined by the point counts in each histogram bin. To encode more descriptive information than point counts, the 3D shape context was extended by summing the lengths of vectors for all points falling in the bin as formulated in Eq. (1).

$$h_{1\le i\le K}(m,n)=\sum_{q\in Q}\| \vec{qp}_i \|, \text{ where}$$

$$Q=\{q\neq p_i : (q_{x,y}-p_{i(x,y)})\in bin(m),(q_{y,z}-p_{i(y,z)})\in bin(n)\} \quad (1)$$

h(m,n) is the extended 3D shape context descriptor for each muscle model. p_i is the i^{th} centroid point obtained, and q are the remaining *K-1* centroid points in the muscle model. m and n indicate a spherical coordinate system (m: 36 bins in horizontal plane, n: 18 bins in vertical plane). x,y,z are the Cartesian coordinates of each centroid point in the muscle model.

b) Compute all possibilities of the corresponding relations between the M0 model and the M1 model: A data preprocessing technique was firstly carried out in the two 3D shape context descriptors obtained in *a)*: the summed vector lengths (i.e., $M0_{1\le i\le K}(m,n)$ and $M1_{1\le i\le K}(m,n)$) in the two descriptors were normalized into a range of 0 and 1, and the normalized value in each bin was recalculated by $M0^{new}(m,n)=\log(1+M0(m,n))$ for discriminating the values between the neighbor points. After the data preprocessing, all possibilities of the corresponding relations between the two muscle models were computed by Eq. (2).

$$C(i,j)_{1\le i\le K;1\le j\le K}=\frac{1}{2}\sum_{u=1}^{m}\sum_{v=1}^{n}\frac{[M1_j^{new}(u,v)-M0_i^{new}(u,v)]^2}{M1_j^{new}(u,v)+M0_i^{new}(u,v)} \quad (2)$$

c) Find the "best" corresponding relation between the two models: the one-to-one point matching between M0 model and M1 model were enforced by minimizing the cost function Eq. (2) using Hungarian method [10]. After found the correspondences, the 3DMCs were measured by the directions and magnitudes of the set of Euclidean vectors, which denote the displacements between pairs of corresponding points as shown in Fig. 1 Step 3.

4) Muscle Tension Estimation:

a) Direction: In this study, the direction of each muscle tension $\vec{D}$ was estimated as the resultant direction of displacements of all sample points within each muscle model,

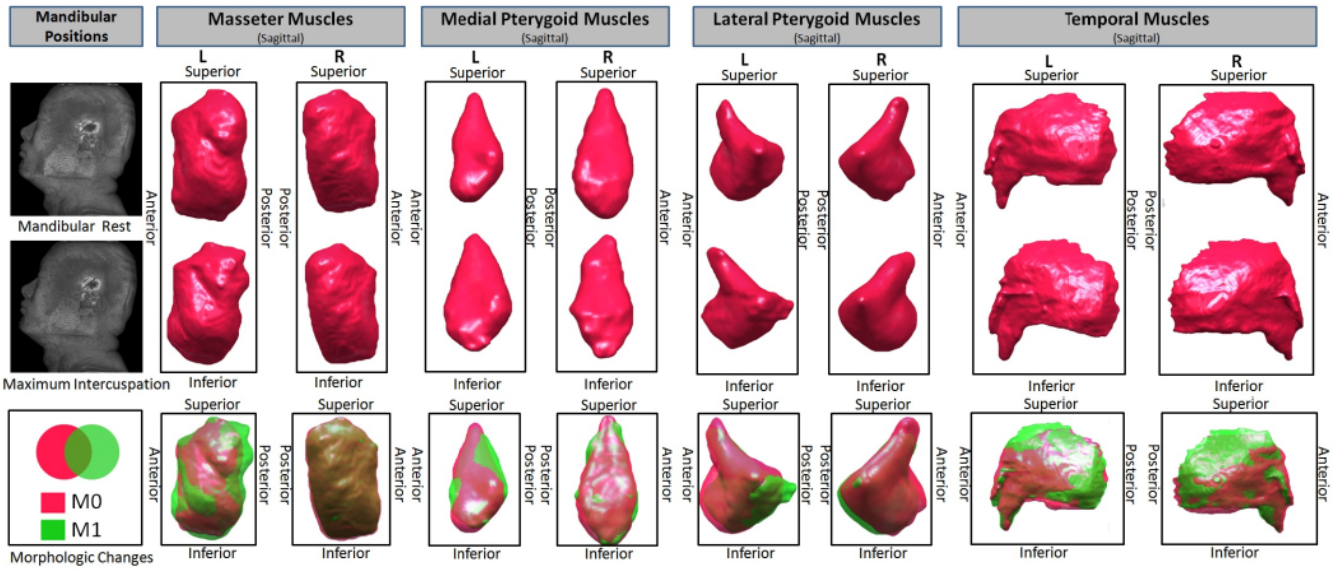

Figure 3. Three-dimensional reconstruction of masticatory muscles.

and was calculated by $\sum_{n=1}^{K} \vec{d}_n / |\sum_{n=1}^{K} \vec{d}_n|$ for each muscle. K is the number of sample points and $\vec{d}_n$ is the displacement of n^{th} sample point.

b) Magnitude: The magnitude of each muscle tension could not be directly measured by current techniques. However, the degree of the muscle deformation (i.e. 3DMCs) and its elastic properties could be used to estimate the muscle tension. In this study, the magnitude of each muscle tension was estimated by Eq. (3).

$$M = \| \sum_{n=1}^{K} \vec{D}_n \| * PFI \tag{3}$$

where the term $\| \sum_{n=1}^{K} \vec{D}_n \|$ is resultant displacement of all sample points for each muscle, and it can describe the degree of muscle deformation since its origin is fixed during mandibular movements. *PFI* [11] (Priority for Force Index) is an index expressing the maximal force of muscle per unit volume under the same amount of maximal work. It was defined by Eq. (4).

$$PFI = PCS / V^{2/3} \tag{4}$$

where *PCS* is the physiological cross-sectional area which was defined as *V/FL* (*FL*: average fiber bundle length), and *V* is the muscle volume. The *PFI* for human masticatory muscles have been investigated by Van Eijden et al., 1995 [12] as Table 1 shows.

Table 1. Priority for force index of the jaw-closing and jaw-opening muscles

	MM	MPM	LPM	TM
PFI	1.39	1.53	0.91	1.24

In order to estimate the magnitudes of muscle tensions for the four group muscles by Eq. (3), the sample points in the four muscle models (MM, MPM, LPM and TM) in the initial condition M0 were assumed to represent the volumes with approximately the same size. i.e., when we sampling the muscle models in II-B-*2)*, the number of sample points in the four group muscles should be based on the following constraint.

$$\frac{V_{MM}}{K_{MM}} \approx \frac{V_{MPM}}{K_{MPM}} \approx \frac{V_{LPM}}{K_{LPM}} \approx \frac{V_{TM}}{K_{TM}} \tag{5}$$

where *V* is the muscle volume and K is the number of sample points.

C. Measurement of Subject-specific Mandibular Movement

The mental protuberance of the mandible was suggested to be a landmark for measuring the mandibular movement since it could be clearly identified in the MR images from the coronal plane as shown in Fig. 2 a. Thereby the mental protuberance was segmented from the two sets of MR images using the same approach with the muscle segmentation (Fig. 2 b).

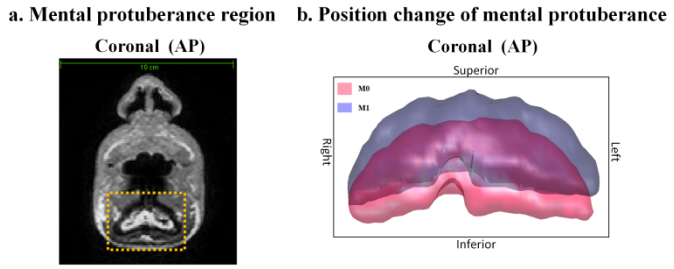

Figure 2. Measurement of subject-specific mandibular movement

III. Experiments & Results

A. Three-dimensional Reconstruction of masticatory muscles

A total of sixteen 3D muscle models under the two mandibular positions were reconstructed and shown in the three anatomic planes (Fig. 3-2^{nd}~3^{th} rows). The intra-rater reliability and inter-rater reliability of the segmentations of the sixteen muscles were very high, with ICC of 0.98 and 0.96,

Table 2. Number of sample points. V: volume; K_1 K_2 and K_3 indicate the numbers of sample points for each muscle at M0 under the same unit volume

M0	MM		MPM		LPM		TM	
	L	R	L	R	L	R	L	R
V(cm^3)	53.15	55.24	15.78	15.10	17.29	15.79	98.09	100.31
Volume=5mm^3								
K_1	425	442	126	121	138	126	785	802
Volume=4 mm^3								
K_2	830	863	247	236	270	247	1533	1567
Volume=3 mm^3								
K_3	1969	2047	584	559	640	584	3633	3715

Table 3. Comparison Results between M_T and M_O under different numbers of sample points

K_1		Dice	SMAD	HD	K_2	Dice	SMAD	HD	K_3	Dice	SMAD	HD
MM	L	86.10%	0.64	3.60		88.21%	0.60	3.23		90.13%	0.52	2.54
	R	85.10%	0.65	4.32		87.5%	0.62	3.70		89.85%	0.50	3.05
MPM	L	88.00%	0.65	3.10		90.10%	0.60	2.64		92.34%	0.50	1.75
	R	86.56%	0.65	3.54		89.22%	0.61	3.06		91.61%	0.52	2.41
LPM	L	87.24%	0.65	3.87		89.22%	0.61	3.10		92.09%	0.50	2.31
	R	87.86%	0.65	3.80		90.03%	0.62	3.15		93.79%	0.50	2.94
TM	L	81.50%	0.91	5.78		85.90%	0.83	4.96		87.57%	0.75	4.46
	R	83.45%	0.84	6.84		87.60%	0.76	6.03		89.30%	0.69	5.52

respectively. For each muscle, the two models before and after mandibular position changed were demonstrated in the same coordinate system by different colors (Fig. 3-4th rows) for observing the morphologic changes. The morphologic changes of the masticatory muscles accompanied by the changes of mandibular position were clearly seen from these reconstructed muscle models, moreover the differentials of the morphologic changes between the left and right muscles were also observed.

B. *Estimation of Masticatory Muscle Tensions*

1) Validation of Recovered Correspondences: In section II, we described an extended 3D shape context method for finding the "best" corresponding points between the M0 model and M1 model for each muscle. To validate the recovered correspondences between the two models, some form of ground truth are required. In this study, the points were sampled uniformly from the muscle volume since the purpose of this study is to investigate the morphologic change of the entire muscle. Therefore the key-points such as maximal of curvature, inflection points or anatomical landmarks were not suitable for assessing the point matching algorithm. Instead, we investigated the qualities of the non-rigid registrations from the M0 to M1 models according to the recovered correspondences since the quality of non-rigid transformation is determined by the accuracy of the recovered correspondences. e.g an incorrect correspondence would misguide the thin plate spline (TPS) transformation leading to unacceptable results. For each muscle, 3D TPS was employed to generate a simulated M1 model based on the recovered correspondences, and then the quality of non-rigid registration was assessed by comparing the morphologic similarities between the simulated M1 model and the original M1 model by using the three parameters: symmetric mean absolute distance (SMAD) [13], Hausdorff distance (HD) and Dice coefficient (spatial overlap). Table 2. shows the numbers of sample points determined by the volumes with different sizes. Table 3 shows the comparison results between the simulated M1 models and the original M1 models. By reducing the volume size for the four group muscles, the global errors in terms of SMAD, HD and Dice were reduced, respectively. As expected, the global errors of the recovered correspondences could be reduced when the number of sample points moderately increased. Since the approximation of the continuous muscle could be improved, meanwhile the local error between the locations of its recovered corresponding point and its physically exact corresponding point could also be reduced.

2) Relationship between Mandibular Movement and Masticatory Muscle Tensions

The measured mandibular movement and the muscle tensions estimated by K_3 (Table 2) were decomposed into the three anatomic planes and shown in Fig. 4. In Fig. 4 a and b, the mandible was moved superiorly and slightly anteriorly (Left: D: 94º, M: 3.30mm). According to the estimated values of muscle tensions, this movement was caused by the three closing muscle groups (MM(L), MM(R), MPM(L), MPM(R), TM(L) and TM(R)), which produced the upward tensions to make the mandible rotate about the horizontal axis as a hinge movement. LPM (LPM(L) and LPM(R)) during the maximum intercuspation were passively stretched by the condyle heads, and hence the LPM were considered to produce a pair of the passive muscle tensions, which only played a role in maintaining the mandibular posture. In Fig. 4 c, the mandible was moved superiorly and slightly to the left side (D: 82º, M: 3.32mm). The upward movement of the mandible could be explained as the aforementioned hinge movement, whereas the slight left movement was due to the unbalanced forces on the left-right axis and the inferior-superior axis, i.e. the horizontal resultant force on the left side mandible was bigger than the horizontal resultant force on the right side Moreover, although the muscle tensions on both sides pulled the mandible

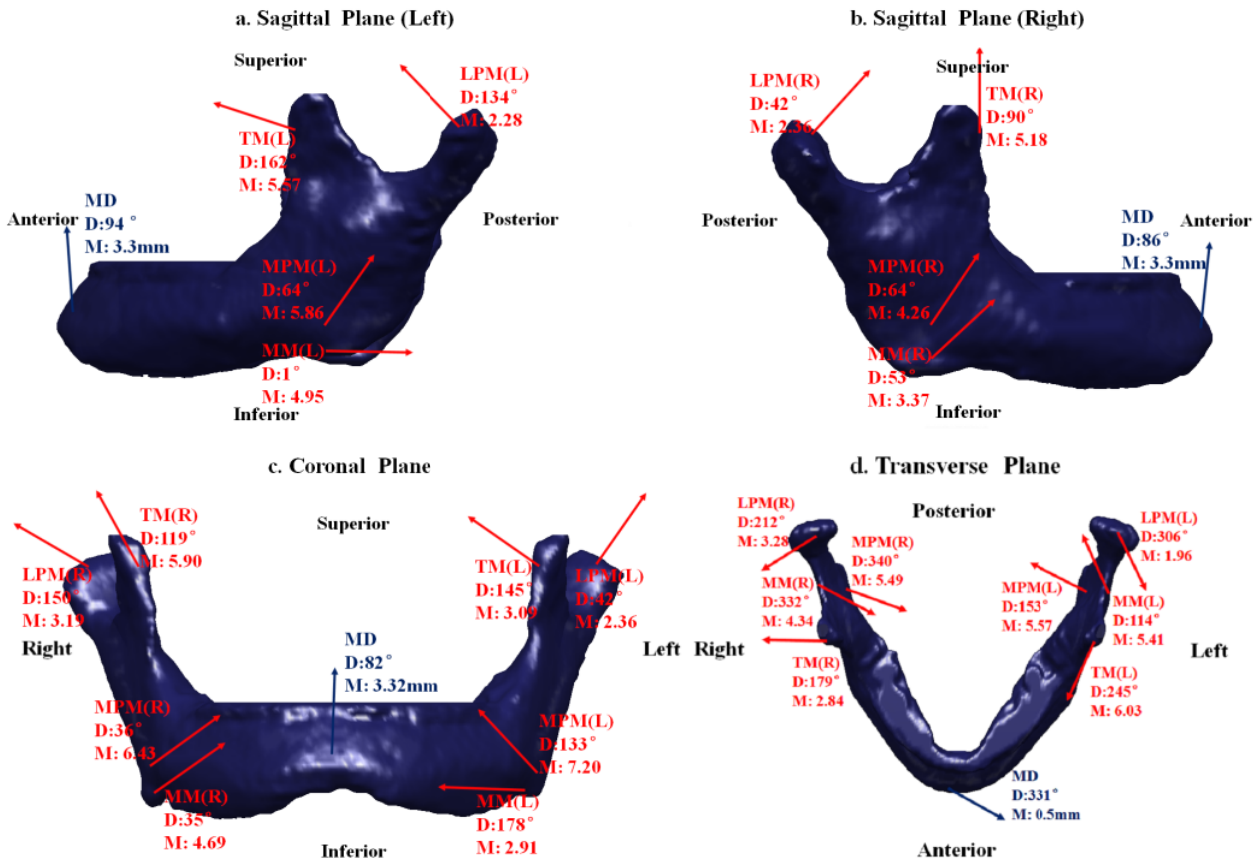

Figure 4. Biomechanical relationship between mandibular movement and masticatory muscle activities. MD: mandible, MM (L): left masseter muscle, MM (R): right masseter muscle, MPM (L): left medial pterygoid muscle, MPM (R): right medial pterygoid muscle, LPM (L): left lateral pterygoid muscle, LPM (R): right lateral pterygoid muscle, TM (L): left temporal muscle, TM (R): right temporal muscle, D: muscle tension direction (0º~360º), M: estimated magnitudes of muscle tensions which were regulated between 0 and 10. For MD, D is the direction of the displacement (0º~360º) and M is the magnitude of the displacement (mm). The locations of the muscle tensions were anatomically determined by their insertions from the MR images. In a, b and c, in order to clearly see the muscle tensions of the MPM(L) and MPM(R), the arrows were positioned on the lateral surface of the mandible. But, in fact, the MPM were inserted into the medial surface of the mandible. These results were calculated according to the numbers of sample points in K_3.

superiorly, the vertical resultant force on the right side was bigger than the vertical resultant force on the left side. Thus, the mandible was slightly rotated to the left side about the antero-posterior axis. In Fig. 4 d, the mandible was slightly moved to the anterior and the left side. The anterior movement was caused by the hinge movement, and the leftward movement was related to the aforementioned rotation about the antero-posterior axis as well as the rotation to the left side about the vertical axis, which was due to the resultant force of the muscle tensions on the right side pulled the mandible anteriorly and the resultant force on the left side pulled the mandible posteriorly.

IV. Discussion

The mandibular movement and the masticatory muscles tensions of the subject were accurately estimated, and the subject-specific biomechanical relationship between the mandibular movement and the muscle activities were explained. The present approach can help to explain the biomechanics of the anatomically and functionally complex masticatory system, and would assist in making proper diagnosis and treatment for masticatory muscle dysfunction. Furthermore, as the results showed, it was not a perfect vertical movement for the mandible due to the unbalanced force relations (discussed in Fig. 4 c and d), thereby such findings would be helpful to study the mastication efficiency [14], the tooth development [15] and the reconstruction of the optimum occlusion of the subject. In the future, we plan to apply our proposed method for investigating the muscle tensions in jaw-opening and chewing cases.

Acknowledgment

This project had been funded by the Singapore Bio-Imaging Consortium. The authors wish to thank the Global Centers of Excellence Program, Japan, for supporting the research collaboration between the National University of Singapore and Osaka University.

References

[1] J.W. MacDonald and A.G. Hannam. “Relationship between occlusal contacts and jaw-closing muscle activity during tooth clenching: Part I,” *J Prosthet Dent*, vol. 52, pp. 718-28, 1984.

[2] C.C. Peck and A.G. Hannam. “Human jaw and muscle modeling,” *Arch Oral Biol*, vol. 52, pp. 300-304, 2007.

[3] Y. Yang, K.W.C. Foong, S.H. Ong, K. Takada and M. Yagi. “A new methodology for studying the functional activity of lateral pterygoid muscle,” *62nd AAOMR Annual Meeting,* Dec 7-10, 2011, Chicago, IL, USA: American Academy of Oral and Maxillofacial Radiology, pp. 67, 2011.

[4] http://www-sop.inria.fr/asclepios/software/MedINRIA/

[5] http://www.itksnap.org/pmwiki/pmwiki.php

[6] D. Maret, F. Molinier, J. Braga, O.A. Peters, N. Telmon, J. Treil, J.M. Inglese, A. Cossie, J.L. Kahn and M. Sixou. “Accuracy of 3D reconstructions based on cone beam computed tomography,” *J Dent Res*, vol. 89, pp. 1465-1470, 2010.

[7] S.P. Lloyd. “Least squares quantization in pcm,” *IEEE Trans. Inf. Theory,* vol. 28, pp. 129–137, 1982.

[8] S. Belongie, J. Malik and J. Puzicha. “Shape matching and object recognition using shape contexts,” *IEEE Trans. Pattern Anal. Mach. Intell*, vol. 24, pp. 509-522, 2002.

[9] M. Kortgen, G.J. Park, M. Novotni and R. Klein. “3D shape matching with shape context,” *In Proc of The 7th Central European Seminar on Computer Graphics*, Budmerice, Slovakia, April 22-24, 2003.

[10] H.W. Kuhn. “The Hungarian method for the assignment problem,” *NAV RES LOGIST Q*, vol. 2, pp.83–97, 1955.

[11] R.D. Woittiez, Y.F. Heerkens, P.A. Huijing, W.H.Rijnsburger and R.H. Rozendal. “Functional morphology of the m. gastrocnemius medialis of the rat during growth,” *J. Morphol*, vol. 187, pp. 247-258, 1986.

[12] T.M.G.J. van Eijden, J.H. Koolstra and P. Brugman. “Architechure of the human pterygoid muscles,“ *J Dent Res,* vol. 74, pp. 1489-1495, 1995.

[13] K.O. Babalola, B. Patenaude, P. Aljabar, J. Schnabel, D. Kennedy, W. Crum, S. Smith, T. Cootes, M. Jenkinson and D. Rueckert. “An evaluation of four automatic methods of segmenting the subcortical structures in the brain,” *Neuroimage*, vol. 47, pp. 1435-1447, 2009.

[14] P. Garcia-Morales, P.H. Buschang, G.S. Throckmorton and J.D. English. “Maximum bite force, muscle efficiency and mechanical advantage in children with vertical growth patterns,” *Eur J Orthod*, vol. 25, pp. 265-272, 2003

[15] M. Kubota, H. Nakano, I. Sanjo, K. Sato, T. Sanjo, T. Kamegai and F. Ishikawa. “Maxillofacial morphology and masseter muscle thickness in adults,” *Eur J Orthod*, vol. 20, pp. 535-542, 1998.